IIER - 767TH INTERNATIONAL CONFERENCE ON RECENT INNOVATIONS IN ENGINEERING AND TECHNOLOGY ICRIET, DOHA, QATAR, DECEMBER 10-11, 2019.

NUMERICAL SIMULATION OF A PERISTALTIC BIORHEOLOGICAL SMART MICRO-PUMP

M. El Gendy[1], O. Anwar Bég[2], Tasveer A. Bég[3], Ali Kadir[2] and W.S.Jouri[2]
[1]Computational Mechanics Consultant, Al Rehab, Cairo, Egypt.
[2]Department of Mechanical/Aeronautical Engineering, Salford University, Manchester, M54WT, UK.
[3] Renewable Energy and Computational Multi-Physics, Israfil House, Dickenson Rd., Manchester, M13, UK.
Emails: mgendy93@gmail.com; O.A.Beg@salford.ac.uk (Presenter); tasveerabeg@gmail.com ; A.Kadir@salford.ac.uk; w.s.jouri@salford.ac.uk

1.INTRODUCTION

- Peristalsis involves the propulsion of physiological fluids via rhythmic contraction of the walls of a vessel. It arises in phloem trans-location in botany, embryonic heart development, blood transport in narrow vessels and intestinal dynamics [ ]. Most physiological fluids including blood exhibit non-Newtonian properties which manifest as deformation-rate dependency, yield stress, viscoelasticity, thixotropy. The high concentration of suspended particles (red blood cells, proteins, nutrients, leukocytes) and their inherent elasticity contribute strongly to non-Newtonian behavior, especially in narrow vessels (micro-circulation). Non-Newtonian effects are therefore also likely to contribute strongly in blood micro-pump dynamics even at low deformation rates. Modern smart pumps are increasingly embracing biological mechanisms [[ ]. In this presentation, 3-dimensional simulations of both Newtonian and non-Newtonian fluids in a peristaltic blood micro-pump are described. The Carreau and power-law models are deployed to characterize rheological behaviour. These formulations can correctly model the Newtonian viscous behaviour via a power law index for the shear rate and includes both dilatant (shear-thickening i.e. viscosity is elevated under increasing shear strain and power-law index exceeds unity) and pseudo-plastic (shear-thinning i.e. viscosity reduces under increasing shear strain and power-law index is less than unity) fluids, the latter being more appropriate for blood flows. ANSYS Fluent [ ] finite volume software is implemented for the simulations. Contour plots for velocity, pressure and vorticity are incorporated. The current work is relevant to providing more realistic numerical simulations of actual peristaltic propulsion hydromechanics in bio-inspired micro-pumps and it is envisaged that it will provide a useful compliment to experimental studies.

2. SMART PERISTALTIC MICRO-PUMP MODEL

- A 3-D model was constructed using the design software AutoCAD. The domain of peristaltic pump model was 9 mm in length and 2 mm in width. The height of the tube leading to the pump outlets measured at 0.2 mm. This geometrical model was imported to ANSYS Fluent Software and the material specifications on the layers were defined. The design was further improved to include an inlet layer of 0.2 mm width to represent the pump inlet surface. Laminar, viscous dominated peristaltic flow is considered in the geometrical micro=pump domain

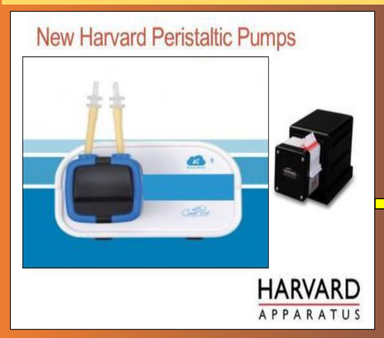

Industrial smart micro-pump

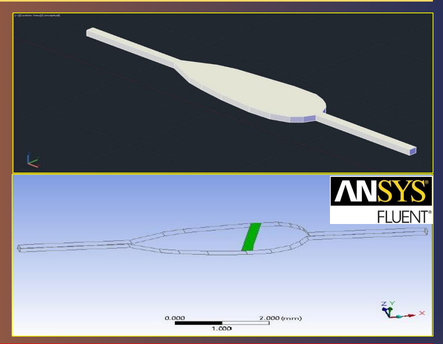

AUTOCAD and ANSYS imported 3-D geometry

The fundamental equations for mass and momentum conservation employed in ANSYS FLUENT are the 3-D unsteady incompressible Navier-Stokes equations which comprise the *mass conservation* and *x-, y- and z-momentum* conservation equations. These may be stated as follows: :

$$\left[\frac{\partial u}{\partial x}+\frac{\partial v}{\partial y}+\frac{\partial w}{\partial z}\right]=0$$

$$\rho\left[\frac{\partial u}{\partial t}+u\frac{\partial u}{\partial x}+v\frac{\partial u}{\partial y}+w\frac{\partial u}{\partial z}\right]=\rho F_x-\frac{\partial p}{\partial x}+\mu\left[\frac{\partial^2 u}{\partial x^2}+\frac{\partial^2 u}{\partial y^2}+\frac{\partial^2 u}{\partial z^2}\right]$$

$$\rho\left[\frac{\partial v}{\partial t}+u\frac{\partial v}{\partial x}+v\frac{\partial v}{\partial y}+w\frac{\partial v}{\partial z}\right]=\rho F_y-\frac{\partial p}{\partial y}+\mu\left[\frac{\partial^2 v}{\partial x^2}+\frac{\partial^2 v}{\partial y^2}+\frac{\partial^2 v}{\partial z^2}\right]$$

$$\rho\left[\frac{\partial w}{\partial t}+u\frac{\partial w}{\partial x}+v\frac{\partial w}{\partial y}+w\frac{\partial w}{\partial z}\right]=\rho F_z-\frac{\partial p}{\partial z}+\mu\left[\frac{\partial^2 w}{\partial x^2}+\frac{\partial^2 w}{\partial y^2}+\frac{\partial^2 w}{\partial z^2}\right]$$

Notation: **(*u,v,w*)** are the velocities in the **(*x,y,z*)** coordinate directions respectively, ***p*** is pressure, $F_x F_y F_z$ are the body forces (gravitational, magnetic, electrical etc), ρ is fluid density, μ is dynamic viscosity, ***t*** is time. The eqns. above are employed in the Newtonian flow simulations. For the non-Newtonian flow simulations, the following modifications are required for viscosity:

$$\mu=\mu_\infty+(\mu_0-\mu_\infty)[1+(\lambda\dot{\gamma})^2]^{\frac{n-1}{2}}$$

Carreau Model: Here μ_0 is the zero shear rate viscosity ($=0.056\ Pa\cdot s$), μ_∞ is the infinite shear rate viscosity ($0.00345\ Pa\cdot s$), λ is the relaxation time (=3.313s), $\dot{\gamma}$ is shear rate (s^{-1}) which is variable and *n* is power law index (= 0.568).

$$\mu=\mu_0*(\dot{\gamma})^{n-1}$$

Power-law model: Here μ_0 * is the flow consistency index (= 0.035 Pa·s), $\dot{\gamma}$ is shear rate (s^{-1}) which is variable and *n* is power law index (= 0.6 i.e. pseudo-plastic). We further note that for the Newtonian simulations, blood has a constant viscosity of $\mu=0.0035\ Pa\cdot s$.

3. ANSYS FLUENT SIMULATION & VALIDATION

A body-sizing meshing approach, compromising mainly of tetrahedron cells to accommodate the anomalous structure of the model, was used to produce an adequate meshing that satisfies the problem specifications. Refinements concentrated at the edges of the inlet and outlets where placed to resolve the complex flow in these zones. The smallest elements were situated at the walls to accommodate boundary layer conditions. The cell distribution around the model can be seen in below. Additionally, refined meshes for the domains were employed to investigate the influence of mesh size on the results for the grid independency study conducted below in Table 1. The results of the grid independency study clearly shows that the values for the outflow velocity stabilizes at around 330,000 elements, with a slight difference in values after that, thus making the original mesh the ideal choice in this situation. The simulations were conducted with the pressure based solver due to the incompressible assumption for blood. The pressure-based solver relies on two types of algorithms, a segregated algorithm and a coupled one. The segregated algorithm uses sequential steps to solve the governing equations in a more memory efficient manner by storing the discretized equations once in the memory. The coupled solver solves the governing equations by coupling them together resulting in a delay in convergence and requiring more memory. Convergence is critical to achieving fast, accurate solutions. Monitoring of the regulated equation residuals of the momentum and continuity equations should preferably be lower than 10^{-5}. However, this criterion alone does not guarantee the effective validity of results. Some of the cases might not fulfill the required residual criterion regardless of the validity of the results, and other cases might yield incorrect solutions even with low residuals. Thus, the monitoring of the mass, conservation and output pressure is required. The total fractional difference between the inward and outward mass flow of the domain should ideally be below 0.01 %, while the outlet pressure and mass flow through open boundaries should remain constant for a number of iterations before settling for convergence. Furthermore validation of the ANSYS Fluent simulations confirms the accuracy of the computations. In the present study, results of the modified peristaltic micro-pump simulation are compared with the experimental work of Rishi Kant *et al.* [ ].Table 2 below shows the experimental results for the flow rate versus the actuating pressure for the optimized design peristaltic micro pump. The values were converted to accommodate the ANSYS fluent parameter requirements and the simulation was conducted for each actuating pressure factor to verify the simulative reliability. Excellent verification of solutions is demonstrated in Table 2. Confidence in the present ANSYS Fluent results is therefore justifiably high. Table 3 shows the boundary conditions used in the CFD simulations.

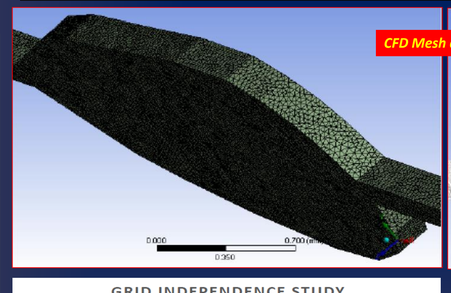

CFD Mesh design

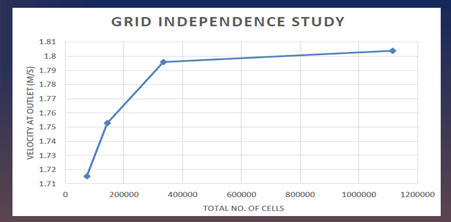

Mesh	Total no. of cells	Total number on Nodes	Velocity at outlet (m/s)	Computational time(minutes)
Double refinement	1114910	204773	1.80382	90
Original mesh	334012	64397	1.795915	20
Half element sizing	143003	28954	1.752749	5
Quarter element sizing	73214	15410	1.715272	2

Table 1: Mesh (grid) independence study

Pressure (Psi)	Experimental Flow rate (µl/s)	Flow rate (µl/s) Present solution (ANSYS Fluent)
0	0	0
2	0.00122	0.0012
4	0.0094	0.00942
6	0.019	0.0188
8	0.025	0.0245
9	0.031	0.030
10	0.036	0.0356
11	0.041	0.0461
12	0.036	0.036

Table 2: Validation with experimental study [6]

Boundary	Condition
Inlet	Pressure -inlet
Outlet 1	Pressure-outlet
Outlet 2	Pressure-outlet
Top wall	Stationary wall with no slip conditions
Bottom wall	Stationary wall with no slip conditions
Side wall 1	Stationary wall with no slip conditions
Side wall 2	Stationary wall with no slip conditions

Table 3: Boundary conditions

Blood is assumed to have constant density of 1050 kg/m³. A steady space pressure solver, coupled with a viscous laminar model, is deployed. All current simulations have been performed using a Lenovo Y510p laptop machine with 8 GB of RAM and an Intel® Core i7-4700MQ CPU @ 2.4 GHz processor with a NVidia® 755m gt SLI GPU running on a Windows 10 platform. The solver was set to include double precision option to allow a higher rate of accuracy and parallel processing option was enabled to utilize the power of the multi core system and the double GPU feature within the machine. The effect of gravity was also taken into consideration with g = -9.81 m/s² along the z-axis. First the velocity distribution along the length of the micro channel was computed. Next the pressure distribution was computed. In addition the vorticity was also computed at specified regions of action around the design of the micro pump. All of the distributions presented were taken along half of the length of the microchannel due to the symmetrical nature of the results on both sides.

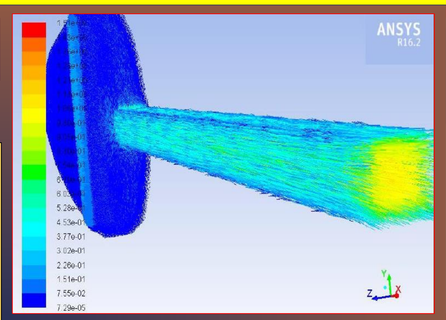

3-D velocity contour plot for blood (power-law non-Newtonian)

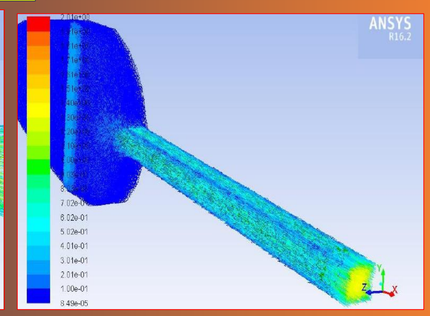

3-D velocity contour plot for blood (Carreau non-Newtonian)

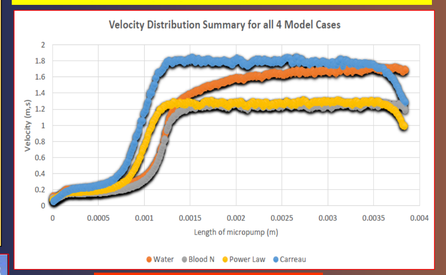

velocity distribution for all 4 cases

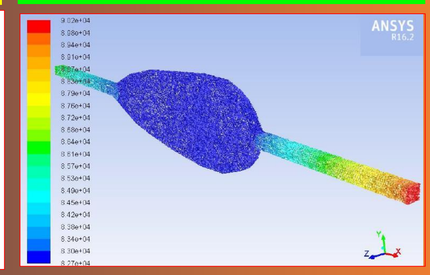

3-D pressure contour plot for blood (power-law non-Newtonian)

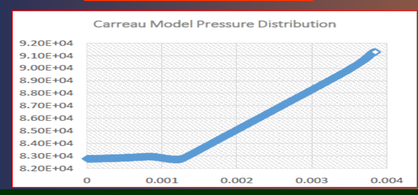

5. DISCUSSION AND CONCLUSIONS

- All cases follow the same trend as the fluid flows from the inlet toward the outlet. They exhibit a sigmoidal velocity growth which is characteristic of micro-pumps An inlet velocity induces a small spike in the velocity profile across the four micro pumps that moves at a steady rate towards the outflow pump at 0.75 mms from the inlet. The micro pump design allows the emulation of the peristaltic action that propels the fluid from the main chamber towards the outlet by the rhythmic contraction of the pump chamber walls. This action induces a large spike in velocity as the fluid moves through the outflow pipe. The highest spike is associated with the non-Newtonian blood flow simulated by the Carreau model as the velocity increased to value of approximately 1.8 m/s. The power law model of the non-Newtonian blood flow showed a similar rate of increase as the Carreau model. However the spike settled at a lower velocity of approximately 1.3 m/s. *Carreau fluid was shown to achieve the best performance and maximum pumping efficiency and indeed is the most robust of the models studied for blood simulation*. The simulations confirm the potential of using peristaltic pumping as an efficient mechanism for transportation of both low and high viscosity fluids. Backflow is eliminated and steady flow profiles are generally maintained along the length of the micro-channel. The results also demonstrate the deviation in response (and hydro-mechanical pumping efficiency) between the power law model and the Carreau model, with the latter attaining more realistic values. The non-Newtonian property of blood i.e. shear thinning, leads to a drop in viscosity. This drop in viscosity is due to the increase in shear strain observed when the fluid moves from the main chamber towards the outflow pipe. This behavior is not seen in Newtonian fluids and thus explains the average rise in speed observed above for the non-Newtonian cases. The figures provide a clear visual representation of the fluid dynamics of 3-D peristaltic pumping. Newtonian blood model achieved lower pressure levels due to its higher viscos nature with a starting pressure of $8.3e^4$ Pa dropping at a higher rate to $7.5e^4$ Pa. The shear thinning behavior, commonly seen in non-Newtonian fluids, results in magnitudes of pressure which deviate significantly from those computed for Newtonian fluids. The starting pressure for both the power law model and the Carreau model remained high at $8.3e4$ Pa and ascended up to $8.95e^4$ Pa for the power law model and $9.13e^4$ for the Carreau model. This once again proved the efficiency of the Carreau model over the Power Law model for peristaltic pumping. Vorticity allows an appreciation of the tendency of a fluid particle to rotate or circulate at a particular point. It also contributes strongly to trapping phenomena in peristaltic fluid mechanics. ANSYS Fluent allows vorticity computation easily via the "flow physics" GUI specifications. For both Newtonian cases, the maximum vorticity was noted at the entrance of the outflow pump from the main chamber achieving values of 83000 (s^{-1}) and 50000 (s^{-1}) for the water and blood respectively. On the other hand maximum vorticity for the non-Newtonian cases was achieved at the outlet with the power model achieving a modest 57500 (s^{-1}) while the Carreau model attained significantly higher vorticity of 85000 (s^{-1}). Future studies will consider magneto-rheological smart pumps which feature electrically-conducting blood properties. [ ]

REFERENCES

- [1[1] D. Tripathi and O. Anwar Bég (2014). Mathematical modeling of peristaltic propulsion of viscoplastic fluids, *Proc. IMECHE- Part H; J. Engineering in Medicine, 228 (1): 67-88.*
- [2] Laser DJ, Santiago JG (2004) A review of micropumps. *J Micromech Microeng* 14:35
- [3] El Gendy M (2016). Investigation of the effect of primary peristaltic transport in Newtonian and non-Newtonian fluids using an optimized micro-pump, *MSc Thesis, Aerospace Engineering*, Salford University, Manchester, UK, September.
- [4] Kant, R., Singh, H., Nayak, M. and Bhattacharya, S., (2013). Optimization of design and characterization of a novel micro-pumping system with peristaltic motion. *Microsystem Technologies*, 19(4), 563-575.
- [5] O. Anwar Bég (2018), Multi-physical electro-magnetic propulsion fluid dynamics: mathematical modelling and computation, *Mathematical Modelling: Methods, Applications and Research, W. Willis and Seth Sparks (Ed), Chapter 1, 1-88 Nova Science, USA..*